Available online at www.sciencedirect.com

ScienceDirect

IFAC PapersOnLine 55-33 (2022) 48–53

Evaluation of robust sensors placement schemes for leaks isolation in water distribution networks

M. Mazzoleni *, M. Scandella **, F. Previdi *

* Department of Management, Information and Production engineering University of Bergamo, via Marconi 5, 24044 Dalmine (BG), Italy (e-mail: mirko.mazzoleni@unibg.it).
** Department of Electrical and Electronic Engineering, Imperial College London, London, United Kingdom.

Abstract: This paper proposes and evaluates robust design schemes for pressure sensors placement and leak isolation in Water Distribution Networks (WDNs). The proposed sensors placement strategy consider the impact of measurements noise and varying water demand at terminal nodes of the network. The best configurations are obtained with a Genetic Algorithm (GA) by optimizing different performance costs. The isolation performance are evaluated in simulation on a Discrict Metered Area (DMA) of a small town in northern Italy.

Keywords: Fault diagnosis; Water networks

1. INTRODUCTION

The search for leaks in water distribution systems is an issue that affects water companies and their customers around the world, causing significant economic losses, third-party damage and health risks (Chan et al., 2018). A first survey work conducted by Thornton (2002) revealed that almost 20% of the US water supply was lost through leaking pipes. More recently, Saqib et al. (2017) reports how in the Kingdom of Saudi Arabia water losses in cities account for around 35% of the total water supply. In Italy, where this work is based, according to the Italian National Institute of Statistics (ISTAT), the amount of water losses corresponds to 37.3% of the country water consumption. These wastes are mainly due to systems ageing, errors in meter measurements and abusive connections, see the ISTAT (2020) report.

It is therefore not surprising how the search for leaks in Water Distribution Networks (WDNs) has attracted a lot of attention from the research community. To tackle the leak detection and isolation task, WNDs are usually subdivided into smaller subnetworks, called District Metered Areas (DMAs). Then, flow and pressure sensors are installed to monitor the network behaviour, typically during night time when water demand is at its minimum (Pérez et al., 2014).

The leak isolation problem in DMAs has been extensively faced in the literature, see e.g. the surveys of Chan et al. (2018); Adedeji et al. (2017); Li et al. (2014). Adedeji et al. (2017) divide the diagnosis methods into externally-based (i.e. with sensing actions from the outside) and internally-based (i.e. with sensors placed internally in the pipes). Chan et al. (2018) propose a classification into passive and active methods. The former ones require a direct visual inspection or monitoring of sites. Active system are based on some measurements (flow, pressure, acoustic, vibration) processing. They can be further classified into transient-based (Colombo et al., 2009), data-driven (Wu and Liu, 2017) and model-based approaches.

The automatic control community vastly contributed to the development of model-based approaches for leak isolation. However, standard techniques of model-based diagnosis, see e.g. Varga (2017); Ding (2013), cannot be straightforwardly applied since the hydraulic model would be composed by a set of nonlinear equations with no explicit solutions. Thus, the hydraulic system at the base of the DMA is often simulated through modeling software such as EPANET (Rossman et al., 2000).

The performance of leak isolation depends on the number of available sensors and their placement in the DMA (Daniel et al., 2022). Thus, the choice of the sensors configuration (their number and placement) is a key issue, considering the trade-off between isolation performance and sensors number (that depends on budget constraints). In this view, pressure sensors are more commonly employed with respect to flow ones due to their cheaper nature. Thus, the typical approach to leak isolation consists of two distinct phases: (i) choice of the sensors configuration (ii) development of a leak isolation algorithm given the chosen sensors configuration.

This two-stage design is advocated by many authors. Pérez et al. (2011) proposed a model-based method based on pressure measurements and leaks sensitivity analysis, where the monitored pressures at certain nodes of the DMA are compared with the simulated pressures. The optimal sensor configuration is obtained by minimizing an isolation error, via Genetic Algorithms (GAs). This approach has been improved in Casillas et al. (2013), where a varying water demand, leak magnitude and a new sensitivity index are considered. Later, Miquel A. Cuguero

10.1016/j.ifacol.2022.11.008

et al. (2017) introduced a clustering method as in Soldevila et al. (2016) to improve the leak isolation performance, and a new cost function to evaluate the diagnosis results.

In this paper, we extend the approach of Pérez et al. (2011) by introducing more robust cost functions for the sensor placement optimization problem, that take into account the measurements noise and varying water demands. We note that Casillas et al. (2013) considers measurements noise only as a *post-treatment* analysis (i.e. after the sensors configuration has been chosen). In contrast, we embed the measurements noise directly in the sensors configuration cost function. The idea of integrating a varying water demand has been investigated in Casillas et al. (2013) and in Cugueró-Escofet et al. (2015), where an approach based on zonotopes is proposed. Here, we evaluate the robustness of the method by considering *both* noise measurements and varying demand in the sensors configuration design problem.

The evaluation of leaks isolation is not straightforward since it depends on the employed sensors configuration. Thus, we define three evaluation tests for assessing the performance of leak isolation, in the following cases:

(1) *single leak in a fixed node* under varying Signal-to-Noise Ratios (SNRs) on the pressure measurements;
(2) *single leak in each node* under varying SNRs;
(3) *single leak in each node* under varying SNRs and *varying water demands.*

The effect of varying SNRs is only briefly investigated in Casillas et al. (2013). Here, we explicitly investigate its effect on the isolation performance that follows the optimized sensors configuration. Simulation results of the proposed cost functions for sensors placement and the proposed evaluations schemes are based on a DMA in northern Italy.

The paper is organized as follows. The leak isolation strategy is described in section 2. The sensor placement optimization problem is presented in Section 3. Section 4 highlights the applicative example used as the basis for this work and shows the proposed results evaluations. Section 5 concludes the paper.

2. LEAKS ISOLATION

The model-based leak isolation presented in Pérez et al. (2011) relies on pressure measurements at network demand nodes and their estimates (performed by the network hydraulic model). Consider a DMA with m nodes and n pressure sensors, with $n \leq m$. We define the *residual vector* $\mathbf{r} \in \mathbb{R}^{n\times 1}$ as

$$\mathbf{r} = [p_1 - \hat{p}_1 \ , \ \cdots \ , \ p_n - \hat{p}_n]^\top , \quad (1)$$

where p_i represents the measurement of the i-th pressure sensor, $i = 1, \ldots, n$, and $\hat{p}_i$ is the corresponding model output from a leakless simulation (e.g. from the EPANET model).

The isolation is performed by comparing the residual vector (1) with the *sentitivity vectors* $\mathbf{s}_j \in \mathbb{R}^{n\times 1}$

$$\mathbf{s}_j = \left[\frac{\hat{p}_1^{f_j} - \hat{p}_1}{f_j} \ , \ \cdots \ , \ \frac{\hat{p}_n^{f_j} - \hat{p}_n}{f_j} \right]^\top , \quad j = 1, \ldots, m. \quad (2)$$

The quantity $\hat{p}_i^{f_j}$ denotes the simulated pressure value in the i-th node when a leak of magnitude f_j is simulated on the j-th node. We denote the simulation of the fault f_j on the j-th node as a *fault scenario* or simply *scenario.*

Leak isolation is performed by finding the vector (2) which is "most similar" with (1) (see Figure 1). One possible way to compare the residual vector with the sensitivity ones is to use the correlation between the residual and sensitivity vectors. For each fault $j = 1, \ldots, m$, we compute the projection indexes

$$\psi_j = \frac{\mathbf{r}^\top \mathbf{s}_j}{\|\mathbf{r}\| \cdot \|\mathbf{s}_j\|}, \quad (3)$$

where $\| \cdot \|$ denotes the Euclidean norm.

A leak is then localized in the node $j^* \in \{1, \ldots, m\}$ when

$$\psi_{j^*} = \max(\psi_1, \ldots, \psi_m). \quad (4)$$

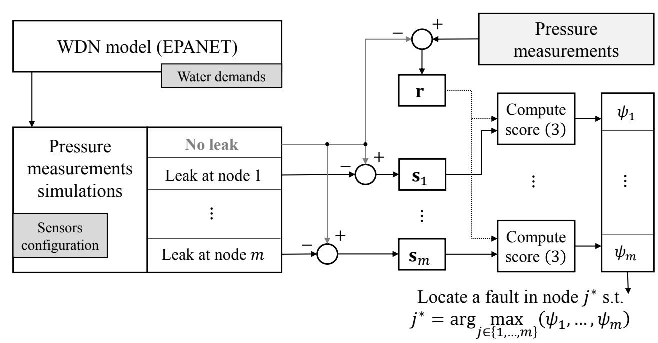

Fig. 1. Leak isolation algorithm. Gray box depicts inputs for other modules.

Remark 1. The discussed approach allows to isolate a single leak at a time in the network.

3. SENSORS PLACEMENT SCHEMES

The performance of the leak isolation ultimately depends on the pressure sensors configuration. The sensors configuration, in turns, has to be robust to variations of: (i) leak magnitude f_j; (ii) measurements noise; (iii) water demand. In this section, we: (i) review the sensors placement problem proposed in Pérez et al. (2011); Casillas et al. (2013); (ii) propose sensors placement schemes that are robust to measurements noise and water demand variations.

3.1 Standard sensors placement

The aim of sensors placement is to find the best placement of a fixed number of sensors, in order to locate a leak in the network as precisely as possible. Since, in this design phase, the pressure sensors are not yet available, a possible strategy is to compute the *simulated residual vector* $\hat{\mathbf{r}}_j \in \mathbb{R}^{m\times 1}$

$$\hat{\mathbf{r}}_j = \left[\hat{p}_1^{v_j} - \hat{p}_1 \ , \ \cdots \ , \ \hat{p}_m^{v_j} - \hat{p}_m\right]^\top , \quad j = 1, \ldots, m \quad (5)$$

where $\hat{p}_z^{v_j}$, $z = 1, \ldots, m$, represents a simulated pressure measurement in the z-th node due to a leak of magnitude v_j in the j-th node. Notice that in (5) we supposed a (simulated) measurement at every node of the network.

Remark 2. The leak magnitudes f_j in (2) and v_j in (5) may differ. Both are user-defined when simulating fault scenarios: a leak magnitude v_j is used when optimizing the sensors placement, while f_j is used when sensors have been placed to perform fault isolation. One can set $f_j = v_j$.

Similarly to (5), we can compute the sensitivity vectors for every node of the networks, so that the quantity in (2) will now be the vector $\hat{\mathbf{s}}_j \in \mathbb{R}^{m\times 1}$

$$\hat{\mathbf{s}}_j = \left[\frac{\hat{p}_1^{f_j} - \hat{p}_1}{f_j}, \cdots, \frac{\hat{p}_m^{f_j} - \hat{p}_m}{f_j} \right]^\top, \quad j = 1, \ldots, m. \quad (6)$$

However, as discussed in Section 2, the number of total nodes m and the number of measured ones n could differ in practice. To this end, define the binary *indicator vector* $\mathbf{q} \in \mathbb{R}^{m\times 1}$ as

$$\mathbf{q} = [q_1, \ \ldots \ q_m]^\top, \quad (7)$$

such that $q_z = 1$ if the pressure at node z is measured, and $q_z = 0$ otherwise, with $z = 1, \ldots, m$. The indicator vector (7) selects only the components of (5) that will be measured by sensor. Let n be the number of deployed sensors. Then

$$\sum_{z=1}^{m} q_z = n. \quad (8)$$

If all nodes will be measured, then $n = m$. From (7), define the *indicator matrix* $\mathbf{Q} \in \mathbb{R}^{m\times m}$ as

$$\mathbf{Q}(\mathbf{q}) = \mathrm{diag}(\mathbf{q}), \quad (9)$$

where $\mathrm{diag}(\mathbf{q})$ indicates the diagonal matrix with the vector $\mathbf{q}$ on the diagonal.

Then, it is possible to compute the projection (3) of the k-th simulated residual in (5) on the j-th sensitivity vector in (2) as

$$\psi_{kj}(\mathbf{q}) = \frac{\hat{\mathbf{r}}_k^\top \cdot \mathbf{Q}(\mathbf{q}) \cdot \hat{\mathbf{s}}_j}{\|\hat{\mathbf{r}}_k \mathbf{Q}(\mathbf{q})\| \cdot \|\hat{\mathbf{s}}_j \mathbf{Q}(\mathbf{q})\|}, \quad k, j = 1, \ldots m. \quad (10)$$

To evaluate the performance of a specific sensors configuration $\mathbf{q}$ in isolating a single leak in any node of the network, the following cost is introduced, (Casillas et al., 2013):

$$\varepsilon(\mathbf{q}) = \frac{1}{m} \sum_{k=1}^{m} \varepsilon_k(\mathbf{q}), \quad (11)$$

where

$$\varepsilon_k(\mathbf{q}) = \begin{cases} 0 & \text{if} \quad \psi_{kk}(\mathbf{q}) = \max\big([\psi_{k1}(\mathbf{q}), \ldots, \psi_{km}(\mathbf{q})]\big) \\ 1 & \text{otherwise.} \end{cases} \quad (12)$$

The rule (12) does not contribute to the error cost when a leak in node k is perfectly located, i.e. when the sensitivity vector $\hat{\mathbf{s}}_k$ is maximally correlated with the simulated residual vector $\hat{\mathbf{r}}_k$. The solution to the "standard" sensor placement problem is obtained by solving (see Figure 2)

$$\min_{\mathbf{q}} \varepsilon(\mathbf{q}). \quad (13)$$

Remark 3. If all possible leaks can be perfectly located by a sensors configuration, then $\varepsilon(\mathbf{q}) = 0$.

The performance of the leak isolation, equipped with the sensor configuration $\mathbf{q}$, decrease due to the presence of noise in the pressure measurements and uncertainty of demand in the nodes. For this reason, we propose two enhancement of the cost (11) in order to obtain more robust sensors configurations against these uncertainties.

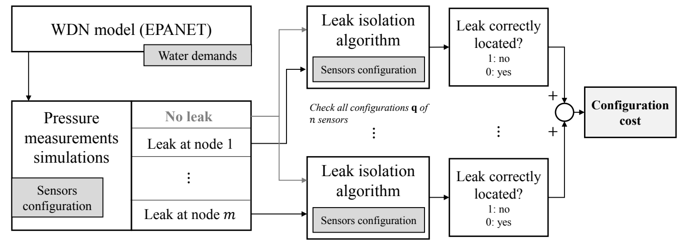

Fig. 2. Standard sensors placement scheme. Gray box depicts inputs for other modules.

3.2 Robust sensor placement against measurements noise

Suppose that an additive gaussian noise $e \sim \mathcal{N}(0, \sigma^2)$ is present on the measurement, where σ^2 is the noise variance. Then, the simulated residual vectors (5) read as

$$\hat{\mathbf{r}}_j(\mathbf{e}) = \left[\left(\hat{p}_1^{v_j} + e_1\right) - \hat{p}_1, \cdots, \left(\hat{p}_m^{v_j} + e_m\right) - \hat{p}_m \right]^\top,$$
$$\mathbf{e} = [e_1, \cdots, e_m]^\top, \qquad j = 1, \ldots, m \quad (14)$$

where $e_z, z = 1, \ldots, m$, denotes the simulated error on the z-th node measurement. The projections can be computed by considering (14) in place of (5) as

$$\psi_{kj}(\mathbf{q}; \mathbf{e}) = \frac{\hat{\mathbf{r}}_k^\top(\mathbf{e}) \cdot \mathbf{Q}(\mathbf{q}) \cdot \hat{\mathbf{s}}_j}{\|\hat{\mathbf{r}}_k(\mathbf{e}) \mathbf{Q}(\mathbf{q})\| \cdot \|\hat{\mathbf{s}}_j \mathbf{Q}(\mathbf{q})\|}, \quad k, j = 1, \ldots m. \quad (15)$$

The cost function with robustness against measurements noise can be defined as

$$\varepsilon(\mathbf{q}; \mathbf{e}) = \frac{1}{M \cdot m} \sum_{w=1}^{M} \sum_{k=1}^{m} \varepsilon_k(\mathbf{q}; \mathbf{e}_w), \quad (16)$$

where, using (15) for the projections ψ_{kj}, we define

$$\varepsilon_k(\mathbf{q}; \mathbf{e}_w) = \begin{cases} 0 & \text{if } \psi_{kk}(\mathbf{q}; \mathbf{e}_w) = \max\big([\psi_{k1}, \ldots, \psi_{km}]\big) \\ 1 & \text{otherwise,} \end{cases}$$

and M denotes the number of Monte Carlo noise realizations. The solution to the "robust against noise" sensor placement problem is obtained by solving

$$\min_{\mathbf{q}} \varepsilon(\mathbf{q}; \mathbf{e}_w). \quad (17)$$

Remark 4. The sensitivity vectors $\hat{\mathbf{s}}_j$ in (15) do not depend on the measurements noise vector $\mathbf{e}$. The noise is added after the simulation only to the residual vectors $\hat{\mathbf{r}}_j$ in (14).

3.3 Robust sensor placement against demand variations

The simulated pressure measurements used in (5) and (14) derive from a single consumption value, typically corresponding to a "standard" or "average" demand. However, since such demand vary over time, it is convenient to find a sensors configuration that is robust with respect to variations of water demand, that causes a change in the pressures. A look at common water consumptions reveals how there are different demands depending on the hour of the day, the day of the week and the season of the year.

Suppose that the water demand varies across T time periods. The simulated noisy residual vectors at a certain time $t = 1, \ldots, T$ can be computed as

$$\hat{\mathbf{r}}_j(\mathbf{e}_t, t) = \left[\left(\hat{p}_{1,t}^{v_j} + e_{1,t}\right) - \hat{p}_{1,t}, \cdots, \left(\hat{p}_{m,t}^{v_j} + e_{m,t}\right) - \hat{p}_{m,t}\right]^\top$$
$$\mathbf{e}_t = \left[e_{1,t}, \cdots, e_{m,t}\right]^\top, \quad j = 1, \ldots, m; t = 1, \ldots T \qquad (18)$$

where $\hat{p}_{z,t}^{v_j}, \hat{p}_{z,t}$ represent respectively the simulated pressure value at the z-th node, at time t, when a leak of magnitude v_j is present on the j-th node, and the when no leak is present. The quantities $e_{z,t}$ are the measurement noises on the z-th node at time t, with $z = 1, \ldots, m$.

Similarly, we can refine the sensitivity vectors (6) to take into account the time variability, for $j = 1, \ldots, m$ and $t = 1, \ldots, T$, as

$$\hat{\mathbf{s}}_j(t) = \left[\frac{\hat{p}_{1,t}^{f_j} - \hat{p}_{1,t}}{f_j}, \cdots, \frac{\hat{p}_{m,t}^{f_j} - \hat{p}_{m,t}}{f_j}\right]^\top. \qquad (19)$$

The improved projections at time t can be computed as

$$\psi_{kj}(\mathbf{q};\, \mathbf{e}_t, t) = \frac{\hat{\mathbf{r}}_k^\top(\mathbf{e}_t, t) \cdot \mathbf{Q}(\mathbf{q}) \cdot \hat{\mathbf{s}}_j(t)}{\|\hat{\mathbf{r}}_k(\mathbf{e}_t, t)\, \mathbf{Q}(\mathbf{q})\| \cdot \|\hat{\mathbf{s}}_j(t)\, \mathbf{Q}(\mathbf{q})\|}, \qquad (20)$$
$$k, j = 1, \ldots m; \quad t = 1, \ldots, T$$

The cost function with robustness against measurements noise and demand variations is thus

$$\varepsilon(\mathbf{q};\, \mathbf{e}, \mathbf{t}) = \frac{1}{T \cdot M \cdot m} \sum_{t=1}^{T} \sum_{w=1}^{M} \sum_{k=1}^{m} \varepsilon_k(\mathbf{q};\, \mathbf{e}_w, t), \qquad (21)$$

where, using (20) for the projections ψ_{kj}, we define

$$\varepsilon_k(\mathbf{q};\, \mathbf{e}_w, t) = \begin{cases} 0 \text{ if } \psi_{kk}(\mathbf{q};\, \mathbf{e}_w, t) = \max\left([\psi_{k1}, \ldots, \psi_{km}]\right) \\ 1 \text{ otherwise,} \end{cases}$$

and $\mathbf{t} \in \mathbb{R}^{T \times 1}$ contains all considered time instants. The solution to the "robust against noise and varying demand" sensor placement problem is obtained by solving

$$\min_{\mathbf{q}} \varepsilon(\mathbf{q};\, \mathbf{e}, \mathbf{t}). \qquad (22)$$

3.4 Optimization with Genetic Algorithms

The best sensors configuration can be obtained by solving the problems (13), (17) or (22). The sensors placement problem is based on the definition of the binary vector $\mathbf{q}$, that defines the number and the location of the pressure sensors, that, in turn, are used to compute the projections and thus the value of the cost function.

Suppose to have a DMA with m nodes and n sensors. Then, the total number of combinations of n sensors is $\frac{m!}{n!(m-n)!}$. An exhaustive search will soon be prohibitive as m and n grows. In these cases, Genetic Algorithms (GAs) are a competing alternative (Banzhaf et al., 1998), where a gene corresponds to the possible presence or absence of a sensor at a given node. Thus, a GA is naturally suited to optimizing over the binary vector $\mathbf{q}$. This approach is also advocated in Casillas et al. (2013); Soldevila et al. (2016); Miquel A. Cuguero et al. (2017).

Remark 5. The use of GA for optimizing sensors placement provides a greedy suboptimal solution with respect to deterministic branch and bound strategies. However, this allows GA to be applied also to cases with hundreds of nodes, as in Pérez et al. (2011).

4. NUMERICAL SIMULATIONS

4.1 Applicative context

The proposed rationales for determining the sensors configuration are motivated by a smart metering project on a WDN in small town in the northern Italy. The project aims at improving the metering ability of the area via the installation of smart meters and algorithms for automatic leaks localization. The town is characterized by a minimum altitude of 172 m and a maximum one of 205 m. A DMA has been selected from the WDN, see Figure 3. The DMA model has been created with the EPANET software. This DMA has a single inlet pipe that supplies water to the district. In this way, the water behavior of the DMA is separated from that of the upstream network (modeled as a reservoir). A leak is simulated by adding an emitter on the node, as suggested in (Rossman et al., 2000, Section 3.1). An emitter is characterized by the discharge Emitter Coefficient (EC) and by the Emitter Exponent (EE). The former can be used to regulate the intensity of the leak and the latter depends on the type of network. In this work, the EE is always set to the default value of 0.5.

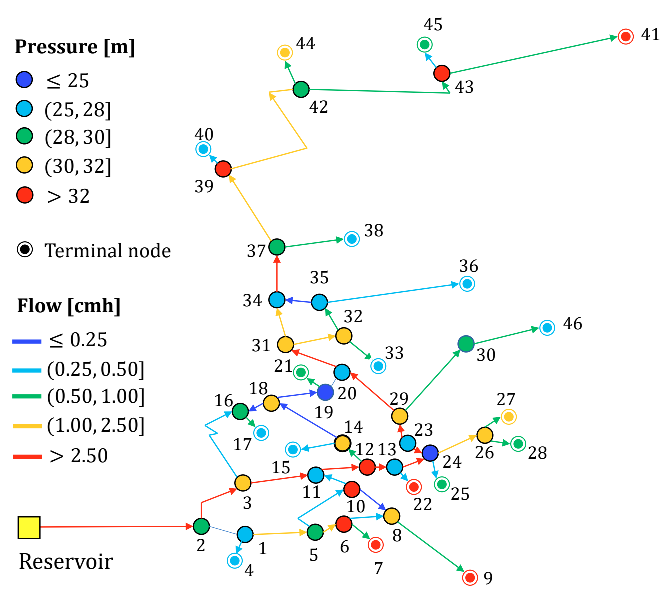

Fig. 3. The considered DMA with $m = 46$ nodes, where 18 of them are terminal nodes. Pressure (in meters, assuming a fluid density of $1000\,\mathrm{kg/m^3}$) and flow range (cubic meters per hour) are depicted.

The outgoing water pressure from the reservoir is set to 3 bar, the typical pressure level present in a pipe of a water system (Tian and Zhang, 2006). The DMA has $m = 46$ nodes. Let the vector $\boldsymbol{\delta} \in \mathbb{R}^{18 \times 1}$ contain the water demands for the 18 terminal nodes (where, in total, 1500 people are connected). The values of $\boldsymbol{\delta}$ are set to the average daily measured demands for each of the terminal node, collected during the winter season. The total demand is $\sum_{d=1}^{18} \delta_d = 14\,\mathrm{m^3/h}$, where δ_d is the d-th component of

$\boldsymbol{\delta}$. Based on budget constraints, the number of sensors is set to $n = 17$ by the company that manages the WDN.

4.2 Evaluation tests

We propose the following tests to evaluate the performance of the sensors configurations in Sections 3.1, 3.2, 3.3, and the relative leak isolation strategy of Section 2:

- **Test 1**: isolation of a single leak in a fixed node at different measurements Signal-to-Noise Ratios (SNRs);
- **Test 2**: isolation of a single leak in all nodes at different measurements SNRs;
- **Test 3**: isolation of a single leak in all nodes at different measurements SNRs and varying demand levels.

Each test is characterized by two different phases: (i) the sensors placement phase; (ii) the leak isolation phase.

Sensors placement phase. The sensors placement phase determines the best sensors configuration, by solving the optimization problems in (13), (17) and (22) for a fixed number of n sensors. For all the tests, we assume an EC coefficient $v_j = f_j = 15$ in (6) and, according to the considered cost, also in (5), (14), and (18). In (17) and (22) we set $M = 1000$ different noise realizations with SNR = 100. We defined $T = 4$ seasonal demands in (18), such that the basic demands at terminal nodes are all multiplied by the following coefficients: 1.5 (spring), 2 (summer), 1.5 (autumn), 1 (winter), see ISTAT (2020).

Leak isolation phase. The leak isolation phase evaluates the performance of the sensors configurations obtained during the sensors placement phase, using the strategy of Section 2. Since the measurements from pressure sensors are simulated, in **Test 1** and **Test 2** we employ (14) in place of (1), while in **Test 3** the vector (18) is used in place of (1). So, all the evaluations employs noisy (simulated) pressure measurements, with SNR $\in \{10, 100, 1000\}$. In fact, real pressure measurements are likely to be noisy.

Genetic algorithm configuration. The parameters of the GA are as follows. We use a population of $\gamma = 20$ chromosomes. The best 4 configurations (natural selection) are mutated with 0.5 probability for each gene. All the configurations go through a uniform crossover that maintains the same number of 1 bits in the chromosome (i.e. number of installed sensors). The GA runs for 250 iterations.

4.3 Test 1: single leak in a fixed node

In this test, a leak v_{14} with EC $= 30\,\mathrm{m}^3/(\mathrm{h}\cdot\sqrt{m})$ is injected only in node 14, so that $v_i = 0, \forall i \neq j$, with $i, j = 1, \ldots, 46$. After the sensors placement phase, the leak isolation phase is executed with $M = 1000$ noise realizations (different from the ones used during the sensors placements), at varying SNRs.

Table 1 reports the isolation performance, across the M noise realizations, on the top three located nodes, using the sensors configurations (13), (17), (22) with $n = 17$. Even if the isolation performance decrease with at lower SNRs, the robust placements outperform the standard one. The correct leaking node is the most frequent answer for all the methods, and when this is not the case, the nearby nodes 15 and 18 are located (see Figure 3). Even if, in this test, there is not a varying demand during the leak isolation phase, the robust placement against varying demand is the best performing approach.

Table 1. Leak isolation performance on node 14, using $n = 17$ sensors with different SNRs (top three located nodes).

Config.	Node	SNR = 1000	SNR = 100	SNR = 10
$\varepsilon(\mathbf{q})$	14	97%	63%	16%
	15	-	21%	29%
	18	-	-	14%
$\varepsilon(\mathbf{q};\, \mathbf{e})$	14	98%	75%	35%
	15	-	17%	28%
	18	-	-	19%
$\varepsilon(\mathbf{q};\, \mathbf{e}, \mathbf{t})$	14	**100%**	**81%**	**41%**
	15	-	12%	26%
	18	-	6%	21%

4.4 Test 2: single leak in all nodes

In this test, a leak v_j with EC $= 30\,\mathrm{m}^3/(\mathrm{h}\cdot\sqrt{m})$ is injected (one leak at a time), in all nodes of the network, $j = 1, \ldots, 46$. Specifically, Test 1 is executed for each leaking node, and the performance are reported in Table 2. Again, the proposed robust configurations performs better than the standard one, in noisy measurements scenarios.

Table 2. Leak isolation performance on all nodes, using $n = 17$ sensors with different SNRs.

Config.	SNR = 1000	SNR = 100	SNR = 10
$\varepsilon(\mathbf{q})$	97.3%	70.6%	30.9%
$\varepsilon(\mathbf{q};\, \mathbf{e})$	97.5%	74.2%	35.6%
$\varepsilon(\mathbf{q};\, \mathbf{e}, \mathbf{t})$	**98.5%**	**82.8%**	**44.3 %**

4.5 Test 3: single leak in all nodes with varying demand

This test consists in running Test 2 for $T = 4$ different water seasonal demands. The goal is to understand if the placements maintain a good capacity to locate the leak in the entire district under different demands.

Table 3 presents the simulation results. The performance are lower than in Table 2 given the additional variability in water consumptions. The standard approach is greatly affected by water demand variations, while the robust approaches are less affected and still performs better in all situations.

In order to better evaluate the robustness of the solution (22), we consider a case where the water demand δ_d varies randomly in $[0.1 \cdot \delta_d, 10 \cdot \delta_d]$ for each terminal node $d = 1, \ldots, 18$. Test 3 is applied with $T = 100$ extractions of water demands and $M = 100$ noise realizations with SNR = 500. Figure 4 presents the average leak location percentage as function of the number of installed sensors. Even in this more involved scenario, the proposed robust approaches attains very good results. Furthermore, it can

Table 3. Leak isolation performance on all nodes, using $n = 17$ sensors with different SNRs and water demands.

Config.	SNR = 1000	SNR = 100	SNR = 10
$\varepsilon(\mathbf{q})$	93.9%	62.6%	27.3%
$\varepsilon(\mathbf{q};\, \mathbf{e})$	96.3%	67.6%	33.8%
$\varepsilon(\mathbf{q};\, \mathbf{e}, \mathbf{t})$	**96.7%**	**76.8%**	**39.8 %**

be noticed how using more than $n = 17$ sensors does not significantly improve the isolation performance of the robust methods.

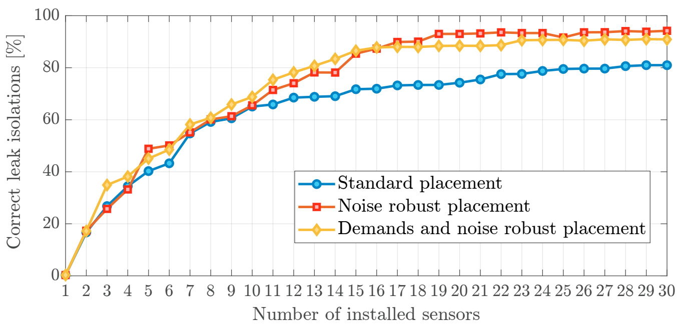

Fig. 4. Isolation performance as function of the number of n sensors installed in the network.

5. CONCLUSIONS

In this paper, we proposed robust rationales for sensors placement in WDN, along with three tests for evaluating the performance of the corresponding leak isolation. The approaches are assessed in simulation on a real DMA, laying the foundations for the practical sensors installation and the development of leak isolation. Next steps will include the evaluation of the methodology with real pressure sensors data.

REFERENCES

Adedeji, K.B., Hamam, Y., Abe, B.T., and Abu-Mahfouz, A.M. (2017). Towards achieving a reliable leakage detection and localization algorithm for application in water piping networks: An overview. *IEEE Access*, 5, 20272–20285. doi:10.1109/ACCESS.2017.2752802.

Banzhaf, W., Francone, F.D., Keller, R.E., and Nordin, P. (1998). *Genetic Programming: An Introduction: On the Automatic Evolution of Computer Programs and Its Applications*. Morgan Kaufmann Publishers Inc., San Francisco, CA, USA.

Casillas, M.V., Puig, V., Garza-Castanon, L.E., and Rosich, A. (2013). Optimal sensor placement for leak location in water distribution networks using genetic algorithms. *Sensors*, 13(11), 14984–15005.

Chan, T.K., Chin, C.S., and Zhong, X. (2018). Review of current technologies and proposed intelligent methodologies for water distributed network leakage detection. *IEEE Access*, 6, 78846–78867. doi:10.1109/ACCESS.2018.2885444.

Colombo, A.F., Lee, P., and Karney, B.W. (2009). A selective literature review of transient-based leak detection methods. *Journal of Hydro-environment Research*, 2(4), 212 – 227. doi:10.1016/j.jher.2009.02.003.

Cugueró-Escofet, P., Blesa, J., Pérez, R., Cuguero-Escofet, M.A., and Sanz, G. (2015). Assessment of a leak localization algorithm in water networks under demand uncertainty. *9th IFAC Symposium on Fault Detection, Supervision andSafety for Technical Processes (SAFEPROCESS)*, 48(21), 226–231.

Daniel, I., Pesantez, J., Letzgus, S., Khaksar Fasaee, M.A., Alghamdi, F., Berglund, E., Mahinthakumar, G., and Cominola, A. (2022). A sequential pressure-based algorithm for data-driven leakage identification and model-based localization in water distribution networks. *Journal of Water Resources Planning and Management*, 148(6), 04022025.

Ding, S.X. (2013). *Model-based fault diagnosis techniques: design schemes, algorithms, and tools, 2nd ed.* Springer Science & Business Media. doi:10.1007/978-1-4471-4799-2.

ISTAT (2020). Istat water statistics, years 2018-2019. URL `https://www.istat.it/it/files/2020/03/Le-statistiche-Istat-sull%E2%80%99acqua.pdf`.

Li, R., Huang, H., Xin, K., and Tao, T. (2014). A review of methods for burst/leakage detection and location in water distribution systems. *Water Supply*, 15(3), 429–441. doi:10.2166/ws.2014.131.

Miquel A. Cuguero, E., Vicenc, P., and Joseba, Q. (2017). Optimal pressure sensor placement and assessment for leak location using a relaxed isolation index: Application to the barcelona water network. *Control Engineering Practice*, 63, 1 – 12. doi:10.1016/j.conengprac.2017.03.003.

Pérez, R., Sanz, G., Puig, V., Quevedo, J., Cuguero Escofet, M.A., Nejjari, F., Meseguer, J., Cembrano, G., Mirats Tur, J.M., and Sarrate, R. (2014). Leak localization in water networks: A model-based methodology using pressure sensors applied to a real network in barcelona [applications of control]. *IEEE Control Systems Magazine*, 34(4), 24–36. doi:10.1109/MCS.2014.2320336.

Pérez, R., Puig, V., Pascual, J., Quevedo, J., Landeros, E., and Peralta, A. (2011). Methodology for leakage isolation using pressure sensitivity analysis in water distribution networks. *Control Engineering Practice*, 19(10), 1157 – 1167. doi:10.1016/j.conengprac.2011.06.004.

Rossman, L.A. et al. (2000). Epanet 2: users manual.

Saqib, N., Mysorewala, M.F., and Cheded, L. (2017). A multiscale approach to leak detection and localization in water pipeline network. *Water Resources Management*, 31(12), 3829–3842.

Soldevila, A., Blesa, J., Tornil-Sin, S., Duviella, E., Fernandez-Canti, R.M., and Puig, V. (2016). Leak localization in water distribution networks using a mixed model-based/data-driven approach. *Control Engineering Practice*, 55, 162 – 173. doi:10.1016/j.conengprac.2016.07.006.

Thornton, J. (2002). *Water Loss Control Manual*. Manuals Series. McGraw-Hill.

Tian, S.j. and Zhang, H. (2006). Study on simulation of hydraulic pipelines' dynamic characteristic by simulink software. *Journal of System Simulation*, 5.

Varga, A. (2017). Solving fault diagnosis problems. *Studies in Systems, Decision and Control, 1st ed.; Springer International Publishing: Berlin, Germany.* doi:10.1007/978-3-319-51559-5.

Wu, Y. and Liu, S. (2017). A review of data-driven approaches for burst detection in water distribution systems. *Urban Water Journal*, 14(9), 972–983. doi:10.1080/1573062X.2017.1279191.